ELSEVIER

Contents lists available at ScienceDirect

Computers, Environment and Urban Systems

journal homepage: www.elsevier.com/locate/ceus





An agent-based modeling approach for public charging demand estimation and charging station location optimization at urban scale

Zhiyan Yi ^a, Bingkun Chen ^b, Xiaoyue Cathy Liu ^{c,*}, Ran Wei ^d, Jianli Chen ^e, Zhuo Chen ^b

- a Department of Civil & Environmental Engineering, University of Utah, 110 Central Campus Dr. RM 1650, Salt Lake City, UT 84112, United States of America
- ^b Department of Civil Engineering, Monash University, Australia
- c Department of Civil & Environmental Engineering, University of Utah, 110 Central Campus Dr. RM 2137, Salt Lake City, UT 84112, United States of America
- ^d School of Public Policy, University of California, Riverside, United States of America
- e Department of Civil & Environmental Engineering, University of Utah, 110 Central Campus Dr. RM 2032, Salt Lake City, UT 84112, United States of America

ARTICLE INFO

Keywords: Electric vehicles Agent-based simulation Charging demand modeling Charging infrastructure Maximal coverage location problem

ABSTRACT

As the market penetration of electric vehicles (EVs) increases, the surge of charging demand could potentially overload the power grid and disrupt infrastructure planning. Hence, an efficient deployment strategy of electrical vehicle supply equipment (EVSE) is much needed. This study attempts to address the EVSE problem from a microscopic perspective by formulating the problem in two steps: public charging demand simulation and charging station location optimization. Specifically, we apply agent-based modeling approach to produce high-resolution daily driving profiles within an urban-scale context using MATSim. Subsequently, we perform EV assignment based on socioeconomic attributes to determine EV adopters. Energy consumption model and public charging rule are specified for generating synthetic public charging demand and such demand is validated against real-world public charging records to guarantee the robustness of simulation results. In the second step, we apply a location approach – capacitated maximal coverage location problem (CMCLP) model – to reallocate existing charging stations with the objective of maximizing the coverage of total charging demands generated from the previous step under the budget and load capacity constraints. The entire framework is capable of modeling the spatiotemporal distribution of public charging demand in a bottom-up fashion, and provide practical support for future public EVSE installation.

1. Introduction

The electric vehicle (EV) market has been progressively growing in the past decade with promising sales records in many countries (Paoli & Gül, 2022). In the United States, for example, the sales of EVs and plugin hybrid electric vehicles (PHEVs) nearly doubled from 308,000 in 2020 to 608,000 in 2021 (US Department of Energy, 2022). In China, EV sales grew by 85% from 2018 to 2019, significantly above the industry average (McKinsey, 2019). Such significant rise in EV adoption rate is attributable to policy incentives, technological advancement, promotion of carbon neutral and net-zero emissions economy, etc. (Debnath, Bardhan, Reiner, & Miller, 2021; Kumar, Chakraborty, & Mandal, 2021; Liu, Sun, Zheng, & Huang, 2021). The ever-increasing EV adoption is beneficial to reducing greenhouse gas (GHG) emissions, supporting the sustainable transport system, and decreasing the reliance on fossil fuels

(Borén et al., 2017). As the booming of EVs creates positive impacts in multiple areas, it brings challenges to the entire society as well.

Among those challenges, the surge of EV charging demand in response to the fast EV adoption could potentially overload the power grid and affect infrastructure planning (Deb, Kalita, & Mahanta, 2018; Deb, Tammi, Kalita, & Mahanta, 2018; Wu, Ravey, Chrenko, & Miraoui, 2019). EV charging can be divided into home charging and public charging depending on charging locations. In the United States, home charging is still the dominant charging mode, accounting for approximately 80% of all charging events (Smart & Schey, 2012). However, public charging plays an indispensable role under several circumstances. First, drivers who often perform long-distance trips would heavily rely on public charging due to the limited mileage range of EVs. Second, home charging requires the charging facilities to be installed at home garage. Yet many existing EV drivers or potential EV buyers may live in

E-mail addresses: zhiyan.yi@utah.edu (Z. Yi), bingkun.chen@monash.edu (B. Chen), cathy.liu@utah.edu (X.C. Liu), ran.wei@ucr.edu (R. Wei), jianli.chen@utah.edu (J. Chen), zhuo.chen1@monash.edu (Z. Chen).

^{*} Corresponding author.

housing units that have no access to a garage or carport. For instance, Ou, Lin, He, and Przesmitzki (2018) estimated that the home parking availability in Shanghai, China was merely 5.3% in 2005. Therefore, augmenting the network coverage of public charging infrastructures can effectively eliminate the resistance to EV purchase. Last but not least, the concept of taxi electrification has been widely expanded in recent years as electric taxi pilots have already been launched in several cities such as New York City, U.S., and Shenzhen, China (Yang, Dong, & Hu, 2018). Considering the much longer daily mileage of taxis, public charging infrastructures appear to be crucial to support such service.

A natural question to address, based on these aforementioned challenges then, is how to optimally place public charging stations to increase demand coverage and sufficiently exploit utilization of the public electric vehicle supply equipment (EVSE). In general, EVSE location problem are often attempted in two steps: public charging demand estimation and public charging station location optimization. Through this workflow, the first step - how to accurately estimate public charging demand - is more challenging because the public charging decision is dictated by a myriad of complex factors, including drivers' charging preference, charging facility accessibility, and EV's remaining state of charge (SoC) (Zhang, Luo, Oiu, & Fu, 2022). Previous studies on public charging demand estimation can be classified into macro- and microlevel approaches. For the macro-level studies, urban informatics and travel mobility information are often utilized to quantify public charging demand in different regions and to extract potential spatial correlation (Dong, Ma, Wei, & Haycox, 2019; Hu, Dong, Lin, & Yang, 2018; Kontou, Liu, Xie, Wu, & Lin, 2019; Tu et al., 2016; Vazifeh, Zhang, Santi, & Ratti, 2019; Yi, Liu, Wei, Chen, & Dai, 2021). In contrast, micro-level approaches mimic EV drivers' daily travel behavior and public charging requests using simulation software in a bottom-up fashion (Adenaw & Lienkamp, 2021; He, Yin, & Zhou, 2015; Lopez, Allana, & Biona, 2021; Marmaras, Xydas, & Cipcigan, 2017; Novosel et al., 2015; Wang & Infield, 2018; Xi, Sioshansi, & Marano, 2013). Compared with macro-level approaches, micro-level methods are capable of producing high-resolution results, such as hourly-level charging distribution, for detailed behavioral analysis. Simulation tools can also model different charging scenarios (e.g. a mix of standard and fast charging events), in an attempt to manage the charging load. Moreover, simulation-based approaches can adopt future changes (e.g. the increase in EV adoption) when assessing the charging demand. For these reasons, micro-level approaches are more suitable to use if high-resolution constraints need be considered for optimizing charging infrastructures.

The majority of existing microscopic methods for public charging demand estimation follow a similar modeling framework, which can be roughly divided into three steps. The first step is to create synthetic drivers and assign them with daily driving profiles to simulate the traffic for the entire study area. This step can be achieved by either populating seed samples from household travel records or generating stochastic activities using Markov chain (Wang, Huang, & Infield, 2014; Xi et al., 2013). The subsequent step is to assign EV drivers that match the current EV adoption rate and its spatial distribution. The final step is to specify EVs' energy consumption model and the public charging decision rule to produce synthetic public charging demands. Although previous studies in general follow such modeling steps, there are a lot of oversimplified assumptions and/or limitations that prevent the model from reproducing accurate spatiotemporal public charging demand portfolios, especially for large-scale (e.g. urban-scale) simulations. Small road networks or simplified network topologies are commonly used for exploring public charging demand considering computational expensiveness (He et al., 2015; Marmaras et al., 2017; Wang & Infield, 2018). However, conclusions from those studies might not be applicable to city-scale analyses, since real traffic patterns vary significantly across geographical areas and interact in a much complex manner. Besides, oversimplification of EV assignment and public charging decision rules can lead to biased estimation of the total energy demand. Several studies assumed a uniform distribution with fixed EV penetration rate to create

synthetic EV drivers (Khan, Mehmood, Haider, Rafique, & Kim, 2018; Wang & Infield, 2018). Yet the decision of EV adoption is driven by miscellaneous factors, including EV model (e.g. mileage range), sociodemographic characteristics (e.g. income, age), and context variables (e.g. accessibility to charging equipment and fuel price) (Javid & Nejat, 2017). Therefore, assumption of random distributions could overlook heterogeneities across neighborhoods and individuals. Apart from EV assignment, simplifying daily activities by confining to only work-based and/or home-based activities in simulation is another limitation (Lopez et al., 2021; Novosel et al., 2015). Places associated with non-workbased activities such as shopping malls, restaurants, entertainment locations, and airports also demonstrate potential public charging needs (Nansai, Tohno, Kono, Kasahara, & Moriguchi, 2001). More importantly, most previous studies were not validated against real-world public charging records, leading to over/under-estimation of the actual public charging demand and inaccurate spatiotemporal charging distribution evaluation. The major hurdle in obtaining public charging data is commercial and/or governmental confidentialities (Wang & Ke, 2018). Without the support of real-world public charging records, the subsequent charging station optimization process would render less

This study aims to optimize the layout of public charging stations at the city-scale by addressing the following two overarching research questions: how to link potential EV users' daily activity patterns with their charging behavior and further estimate the spatial distribution of public charging demand? and Once an estimated charging demand distribution is accomplished, how to optimize the layout of public charging stations such that the overall public charging demand is maximized? Specifically, Salt Lake City (SLC) metropolitan area is selected as a pilot. Utah is the fourth fastest growing state in the U.S., and the population is forecasted to double over the next 20 years. The SLC metropolitan area is home to >80% of the state's population, and surprisingly experiences some of the worst air quality in the nation. As such, there is growing political consensus to address air quality, and PEVs offer a viable solution. The state has aggressive plan in terms of charging station deployment over the next several years and understanding how drivers' daily activities interact with public charging demand at city-scale is paramount to the EV charging station deployment. The modeling framework and findings therefore could provide valuable guidance to regions or areas with similar interests in accelerating EV adoption.

As for the modeling process, we first create the synthetic public charging demand within an urban-scale context in a bottom-up fashion via agent-based modeling. Specifically, Multi-agent Transport Simulation (MATSim), an open-source framework for implementing large-scale agent-based transport simulation, is adopted to model the daily activities of all drivers. We then distribute the EV drivers based on socioeconomic attributes, and further specify the public charging decision rule for generating synthetic public charging demand post-simulation. In the second step, an optimization framework - capacitated maximal coverage location problem (CMCLP) - is formulated based on the generated public charging demands from the previous step. The CMCLP model reallocates existing public charging stations in the study area by maximizing the coverage of total charging demand under the investment cost and load capacity constraints. Note that within the entire framework, synthetic public charging demand is validated against real-world charging records, and optimized charging station deployment is assessed by a plug-in from MATSim that supports the public charging behavior analysis. In sum, the main contributions of this paper are threefold:

 A city-scale agent-based simulation is developed to produce daily travel profiles using time-inhomogeneous Markov chain, and location mapping technique using publicly available data. EV assignment and public charging decision modeling are subsequently specified in post-simulation analyses using socioeconomic and demographic information to produce high-resolution public charging demand;

- The spatiotemporal distribution of synthetic charging demand is validated against real-world public charging records, which are obtained using a dynamic crawling pipeline. The result indicates a consistent charging pattern between synthetic charging demand and actual energy consumption for most areas; and
- The CMCLP model is applied to optimize the deployment of public charging stations taking into consideration both standard and fast charging demands. The capacity constraint is formulated at different hours-of-the-day to ensure charging demands are satisfied even during peak hours. The results can provide practical guidance for future public EVSE installation.

The remainder of this paper is organized as follows. Next section will comprehensively discuss literature related to simulation-based public charging demand analyses, agent-based modeling, and charging station locations optimization problems. Following that, data sources are described in detail. *Methodology* section presents the micro-level modeling framework for public charging demand generation and mathematical formulation of CMCLP model. The *Results and Analysis* section presents the simulation results, charging demand analyses, and optimization outcomes. Conclusions are outlined at the end.

2. Literature review

2.1. Simulation-based public charging demand modeling

Microscopic simulation-based approaches model the public charging demand generation in a bottom-up fashion. One of their major advantages is the ability to reproduce complex traffic situations within large-scale networks and enable operational outputs at the link or intersection level while accounting for the impacts of localized activities. Besides, microscopic modeling produces detailed trip trajectory at the individual level, which can be used for high-resolution analysis. Moreover, the animation and graphic user interface allow researchers to vividly interpret the impact of drivers' daily activities on public charging behavior.

In general, simulation-based approaches for generating public charging demand follow three steps: simulating the daily traffic for the entire study area, assigning EVs among drivers, and specifying energy consumption model and public charging decision rules. The first step can be achieved using simulation software, while the remaining steps can be performed as post-simulation analysis. To model daily traffic, all drivers' household distribution and their daily driving profiles are required. This process can be further separated into population synthesis and stochastic daily activity generation. Population synthesis refers to the use of sample population data to generate a set of households and persons representing the entire population in the modeling region (Paul, Doyle, Stabler, Freedman, & Bettinardi, 2018). Besides, marginal distributions of socioeconomic and demographic characteristics are fed into population synthesizer together with the sample data to create heterogeneous households and individuals. As for stochastic daily activity generation, a common approach is to apply Markov Chain Monte Carlo (MCMC) simulation. For example, Wang et al. (2014) applied a time-inhomogeneous Markov chain to simulate driving patterns based on the UK 2000 Time Use Survey data, a real-world high-resolution dataset that records activities for households' individuals on a 10-min basis. Four states including "driving", "parking at home", "parking at workplace", and "parking at other places" are defined in the Markov chain for the privately owned EVs to estimate the impact of workplace charging during weekday on power grid. Once the synthetic population and their daily activity trips are generated, simulation software can be used to model the traffic of study area with road network information. Following that, a post-simulation analysis can be conducted to assign EV users and distribute public charging demands according to a specified charging decision. A simple strategy for EV assignment is to distribute EV drivers using uniform distribution with a fixed EV penetration rate

ranging from 1% to 100% (Khan et al., 2018; Wang & Infield, 2018; Xi et al., 2013). However, EV adoption is influenced by a myriad of factors, including demographic, contextual, and other types of attributes. The assumption of uniform distribution would ignore the socioeconomic and demographic distinctions across geographical areas, leading to biased EV adoption spread and incorrect charging demand distribution. To estimate EV adoption probability, Javid and Nejat (2017) developed a logistic regression model that considers socioeconomic factors and context variables, such as age, income, and fuel price. After EV assignment, energy consumption model and public charging decision behaviors should be established to determine when and where public charging events occur. The public charging decision rule is relatively difficult to model since drivers' charging preference, charging accessibility, and remaining SoC are challenging to be captured precisely (Herberz, Hahnel, & Brosch, 2022). In previous studies, the attributing factors for modeling public charging include SoC, activity duration, and walking distance to the charging facilities. Researchers generally set a threshold value for each factor according to published reports to trigger public charging events with different logics (Hu et al., 2018; Wang et al., 2014; Zou, Wei, Sun, Hu, & Shiao, 2016).

After performing the aforementioned three steps (daily traffic simulation, EV assignment, and energy consumption and charging decision), the generated synthetic public charging demands can be represented using points. Each demand point is associated with a charging start time, duration, charging type, and location information. This information will be further utilized in the optimization framework for optimizing the public charging station locations.

2.2. Agent-based modeling

Note that there are multiple ways for conducting daily traffic simulation based on the synthetic population and their daily activity trips. Among them, agent-based model (ABM) is one of the widely used approaches. ABM contains a collection of agents or units, and agents can be assigned with different daily activities. The agents will operate according to plans and interact mutually to produce a complex scenario, such as road traffic (Macal & North, 2009). ABM provides a natural description of a system that is highly flexible. It enables the creation of complex simulation environments by inserting heterogeneous units with a variety of attributes, such as age, vocation, and income level. Popular agent-based modeling tools for traffic analysis include Transportation Analysis Simulation System (TRANSIMS) (Smith, Beckman, & Baggerly, 1995), Simulation of Urban Mobility (SUMO) (Krajzewicz, Erdmann, Behrisch, & Bieker, 2012), and MATSim (Axhausen, Horni, & Nagel, 2016).

MATSim is an open-source framework for implementing large-scale agent-based transport simulations. It is arguably the one with the least focus on traffic flow realism but with the highest computing speed and the best behavior model on trip planning. In a nutshell, a synthetic driver (i.e. agent) will perform trip activities within a day, and tries its best to optimize its daily schedule by adjusting possible activities based on a co-evolutionary principle iteratively. Because MATSim is written in Java, it supports a variety of plug-in packages for public charging behavior analyses (e.g. BEAM and DVRP) (Maciejewski & Nagal, 2007; Sheppard, Waraich, Campbell, Pozdnukov, & Gopal, 2017). MATSim requires population distribution, daily activities, road network, and facility locations as inputs. Novosel et al. (2015) applied MATSim to model the hourly distribution of energy consumption of EVs on an urban scale in the cities of Croatia to test their charging impacts on the entire energy system. This study assumed that activities only occur between home and work, and the spatial distribution of home and work locations are estimated based on the socio-demographic data. Adenaw and Lienkamp (2021) applied MATSim to analyze the charging station utilization and user behavior by inserting EVs and charging stations in the simulation environment. The numeric results are tested and verified using a case study in the city of Munich, reflecting realistic spatiotemporal

charging patterns. Furthermore, they encapsulated their work to an open-source framework – UrbanEv-Contrib – based on MATSim, which can serve as a sandbox validating optimized charging infrastructure designs in a dynamic simulation environment.

2.3. Public charging station locations optimization

Public charging infrastructure deployment problem can be solved using location approaches, which contain two components: demand representation and location model. Charging demand can be represented as points, polygons, or flows depending on the specific contexts, and the location model is an optimization framework designed to select the best locations with the goal of maximum utility coverage, minimum cost, or other objectives (Dong et al., 2019; Huang, Kanaroglou, & Zhang, 2016). Demand is considered being covered if it is within a certain travel distance to a charging station. Standard location models include the flow capture location model (FCLM) (Hodgson, 1990), maximal coverage location problem (MCLP) (Church & ReVelle, 1974), and p-Center (Hakimi, 1964).

Among them, the MCLP model is computationally efficient and suitable for problems with demand representation as points or polygons. The MCLP seeks to maximize the target (i.e. charging demand) covered within a desired service distance by locating a fixed number of facilities (i.e. public charging stations). It has been widely adopted for solving the EVSE location problem. Dong et al. (2019) optimized the placement of charge point infrastructure by formulating a MCLP model with the objective of maximizing total demand coverage under the investment budget constraint. One potential flaw of the MCLP model is that the energy capacity for charging ports is not considered. Failing to set capacity limits can lead to an overestimation of service level. To fix this problem, the CMCLP model is developed to refine constraints. Yi, Liu, and Wei (2022) utilized the CMCLP model to optimize the layout of public charging stations on a city scale. Accumulated daily capacity for each charging port and total investment budgets are set as constraints. With finer granularity, hourly charging capacity can be modeled to satisfy the charging demand during peak hours (Tu et al., 2016). The aforementioned MCLP/CMCLP-based charging station optimization models (Asamer, Reinthaler, Ruthmair, Straub, & Puchinger, 2016; Dong et al., 2019; Tu et al., 2016; Yi et al., 2022) attempted the problem from a macro-level, where the entire study area are discretized into grids or polygons, and charging stations are sited onto those cells instead of pinpointed the exact geographical locations. Such discretization will induce low-resolution optimization results because the size of cells can be as large as 1 km by 1 km (Yi et al., 2022). Failing to pinpoint the exact location of charging facilities might provide less practical or useful guidance for detailed infrastructure planning. The ABM can effectively address this problem as it is capable of producing vehicle trajectory records and high-resolution charging requests.

Our study employs CMCLP to maximally capture the public charging demands in the study area under the investment budget and different hours-of-day capacity constraints. Moreover, fast charging demand is incorporated on top of standard charging demand in the optimization framework to present a more realistic charging infrastructure design.

3. Data

A realistic urban-scale simulation requires high-quality inputs. The modeling framework presented in Fig. 1 consists of a series of building blocks. In each building block, methodology (will be explained in the next section) and required data resources are highlighted. First, population and socioeconomic attributes are used for synthetic population generation, and ATUS data is utilized to create time-inhomogeneous Markov chain. Following that, POI and historical OD data are used for location mapping. To execute agent-based simulation via MATSim, road network information is fetched from Open Street Map (OSM). EV assignment and public charging behavior modeling are subsequently performed. Finally, real-world public charging observations is used to validate simulation results, while an optimization model is further implemented based on the simulation results to reallocate the charging stations with maximum coverage of public charging demands. The detailed description for each dataset is explained in the following subsections.

3.1. American time use survey (ATUS)

High quality data is essential to guarantee accurate stochastic behavior modeling for agent-based simulation. Time use survey data has been widely used to model stochastic behaviors of people due to the high resolution of activity information. Hence, we employed ATUS dataset to create synthetic agents. ATUS dataset is collected annually by U.S. Bureau of Labor Statistics, which provides nationally representative estimates of how, where, and with whom people spend their time. Each respondent interviewed by ATUS is documented with demographic information, household status, and daily activity records. To reflect how people spend their time, respondents are asked to collect a detailed account of their activities regarding the type, duration, and location of activities, starting at 4:00 AM the previous day and ending at 4:00 AM on the interview day. We use ATUS data spanning from 2013 to 2017 with approximately 55,000 respondents during weekdays to construct the Markov chain for stochastic daily activities generation.

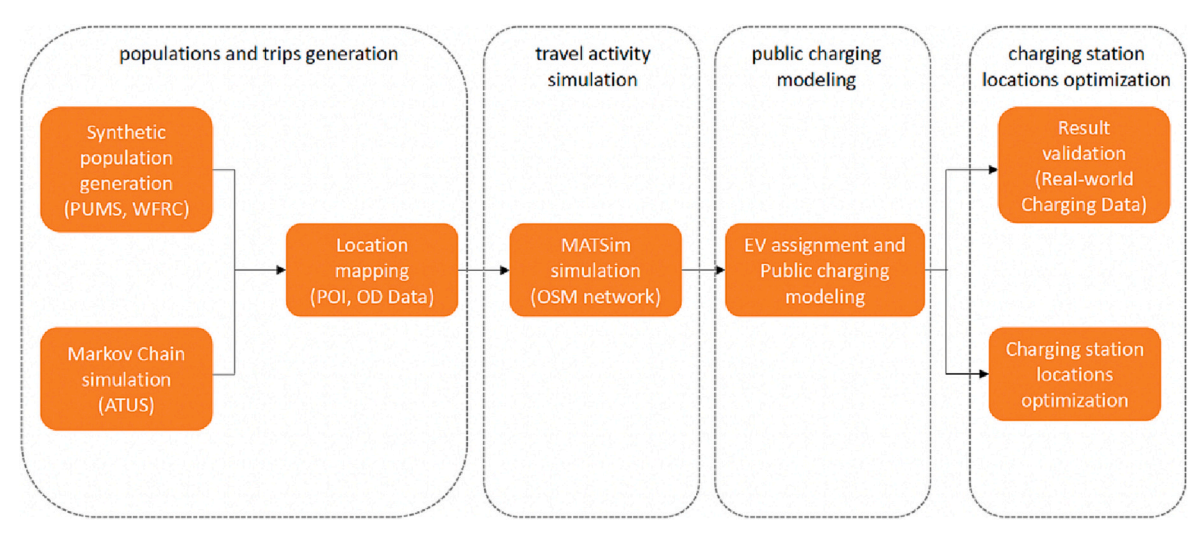


Fig. 1. Model development framework.

3.2. OSM road network information

We extract road network using OSMnx, a python package allowing to download, visualize, and analyze geospatial data from OSM as the required input for MATSim (Boeing, 2017). The representation of a road network in OSM is essentially a directed graph, where edges represent roads and nodes represent conjunction points or dead end of roads. Each road contains the topological information such as coordinates of start and end point, the line string geometry, and length. Moreover, each road is assigned with traffic attributes such as road class, number of lanes, and maximum speed, which are required attributes for MATSim. There are 94,742 roads and 37,766 conjunction points (or dead ends) in total within study area. Roads attributes with missing values are replaced by mean values of all roads within the same road class.

3.3. Sociodemographic information

Synthetic population generation requires two inputs - sample seed and attributes' marginal distributions -to create entire population in the study region. Population sample from Public Use Microdata Sample (PUMS) - a set of records from individual people or household units with disclosure protection enabled (United States Census Bureau, 2019) - is used as sample seed. There are 4924 households and 13,768 persons in the seed population. Each sample household contains attributes including household size, household income, vehicle ownership, and location information. Apart from sample seed, marginal distributions of the aforementioned attributes are required. This study applies TAZ-level socio-demographical information with fine granularity to create realistic simulation scenario. Household distribution, vehicle ownership and average household income in each TAZ are retrieved from Wasatch Front Regional Council (WFRC) to build the marginal distributions of sample's attributes at TAZ level (Wasatch Front Regional Council, 2021). Besides, historical OD distribution data among TAZs is fetched for location mapping purpose.

3.4. Point of interest (POI) data

POI data can effectively reflect urban context and infer people's trip purposes. To extract POIs in our study area, we use Google Place API (Google Place API, 2021). After eliminating unrelated type of POIs (e.g. hotel), there are 59,112 POIs classified in nine categories. The detailed information of classified POI data is shown in Table 1. The POI information is retrieved for the location mapping purpose. Each category of POIs is associated with a specific daily activity as observed in the Activity column.

3.5. Real-world public charging data

The real-world charging data is crawled from ChargePoint, an online application that assists EV users to navigate and review nearby charging sites (Charge Point, 2021). ChargePoint operates the largest online network of independently owned EV charging stations, operating in fourteen countries worldwide. The data crawling period spanned from

Table 1
Description of POI data.

POI ID	Category	Label Examples	Count	Activity
1	Business	office, personal business	23,472	Work
2	Health	hospital, health, doctor	8982	Others
3	Finance	agency, finance building	6691	Work
4	Retail	supermarket, grocery store	10,066	Shop
5	Restaurant	restaurant, food delivery	2181	Dine in
6	Education	school, university	1290	Others
7	NGO	church, government building	1591	Work
8	Entertainments	park, salon, bar, zoo	2422	Others
9	Service	post office, gas station, laundry	2427	Others

Nov 5th, 2020 to Dec 12th, 2020, and the construction steps for dynamic crawling pipeline can be found in (Yi et al., 2022). To sum, there are 109 public charging stations with 516 Level 2 charging ports recorded by ChargePoint that broadcast real-time utilization information (i.e. number of in-use ports at current time point) in the study area. The energy consumption at a certain period for a charging station is calculated as the total number of in-use ports multiplied by the corresponding power of the ports and crawling interval (set as 10 min). The accumulative energy consumption (kWh) during each interval is then summed up across the entire crawling period as the total charging energy consumption. Spatial distribution for 109 charging stations is displayed in Fig. 2, with the height quantifying the cumulative energy consumption within the data collection period.

4. Modeling framework

To simulate EV mobility and associated energy consumption in a high spatiotemporal resolution, the modeling framework in Fig. 1 is divided into four major components: populations and trips generation; travel activity simulation; public charging modeling; and charging station location optimization. We begin by creating synthetic population using sociodemographic information at the traffic analysis zone (TAZ) level. In the meantime, a time-inhomogeneous Markov chain is trained using ATUS data to produce stochastic daily activities. Following that, a location mapping technique is proposed to project those daily activities onto specific geographical locations based on historical travel patterns, POI, and population information. These aforementioned inputs are then fed into MATSim, together with road network, to return the optimal travel plans for all drivers. Upon MATSim simulation result, we apply EV adoption probability model and EV energy consumption model to determine EV distribution and potential public charging demands. This is validated against real-world public charging observations. An optimization model is then employed to maximize the coverage of public charging demand under various constraints.

4.1. Synthetic population generation

Synthetic population generation is the very first step of activitybased modeling. The generated synthetic population should be able to represent person- and/or household-level attributes of the actual population in the modeling region. PopulationSim (Paul et al., 2018), an open-source population synthesizer, is employed for the purpose of this study. Typically, PopulationSim requires three datasets as the inputs: household and person samples with related sociodemographic attributes, and the marginal distributions of controlled variables (e.g., household size and household income). Then PopulationSim utilizes the samples and marginal distributions to generate tables of person and households representing the entire population of the modeling region. The population synthesis in PopulationSim involves two steps: fitting and generation. During the fitting step, entropy maximization is applied to preserve the distribution of initial weights while matching the marginal controls. Once the weights have been assigned for seed sample, the generation step expands the sample using Monte Carlo sampling and optimization-based algorithm. Table 2 gives an example of input data for PopluationSim, comprising the population sample (household and person), and marginal distributions of household size (HHSize), household income (HHInc), and household vehicle ownership (HHVeh) in TAZs. Note that the population sample data in PUMS is aggregated by public use microdata areas (PUMAs) - the special nonoverlapping areas that partition each state into contiguous geographic units containing no fewer than 100,000 people each, to protect privacy.

PopulationSim allows reallocation of population from a larger geographic unit into a smaller one, such as from PUMAs to TAZs. The final outputs from PopulationSim contain synthetic populations and households with corresponding attributes at located TAZs in the study region.



Fig. 2. The spatial distribution of current public charging stations in Salt Lake City metropolitan area.

4.2. Time-inhomogeneous Markov chain

Vehicle movement is a series of state transitions throughout a day. Markov chain is a stochastic model describing a sequence of possible events. Time-inhomogeneous Markov chain refers to chains with different transition probability matrices at each time step. In this study, ATUS data is utilized to construct the sequence of transition matrices for time-inhomogeneous Markov chain. We set time resolution as 10 min (i. e., 144 time steps for an entire day) when use a discrete Markov chain to describe people's daily activities. Such resolution is preferred for detailed analysis of vehicle activities, and trips of short distances (Wang et al., 2014). Specifically, drivers' daily activities are classified into 6 categories: "drive," "stay home," "work," "shop," "dine in," and "others." The indexed activities and state transition relationship are described in Fig. 3(a). Fig. 3(b) describes the transition probability at a specific time t. For example, if t = 48, then p_{02}^{48} denotes the probability from "drive" to "work" at 8:00 AM. Note that the transition between any two different states must be accomplished via "driving" activity, which means that the transition probability between two nondriving states, such as p_{21}^t , is always zero. This assumption is made because we are only interested in the activities that are connected by driving to explore EVs' potential charging opportunities at different locations.

To demonstrate the functionality of this Markov chain, each respondent's daily activity trajectory is first mapped to the state code in Fig. 3(a), and then subsequently transformed to a list representation with the length of 144, where each number in the list denotes an activity code (10-min resolution) at a specific time step. The transition probability p_{ij}^t in stochastic matrix at time step t is calculated as the number of respondents switching from activity i to j at time step t+1 divided by the total number of respondents. Once 143 stochastic matrices (a daily activity list contains 144 time steps) are obtained, we can use them to create a list of synthetic daily activities given the initial states as inputs. The initial state (i.e. activity at 12:00 am) for each person is determined by randomly sampling from a predefined probability density function at t=1.

4.3. Location mapping

Stochastic activities generated by Markov chain do not have geographical location information. Yet agent-based models such as MATSim requires detailed trip information. Therefore, we developed a location mapping strategy to project abstract activities to specific trips with geo-location labels using historical trip distribution and POI data. The proposed location mapping strategy is detailed as follows:

Table 2Sample input data for PopulationSim.

(a) Population sample at PUMA level					
Household id	PUMA id	HHSize	HHInc	HHVeh	
1	35,001	2	50,000	2	

Person id	Household id	PUMA id	Age	Gender
1-1	1	35,001	51	male
1–2	1	35,001	46	female

(b) Marginal distributions of controlled variables in TAZs					
TAZ id	695	712			
PUMA id	35,001	35,001			
Categories of HHSize					
HHSize = 1	174	97			
HHSize = 2	109	137			
HHSize = 3	75	221			
HHSize = 4	34	220			
HHSize = 5 105 22					
HHSize = 6	86	125			
$HHSize \geq 7$	75	219			
Categories of HHInc					
$HHInc \leq 21,297$	$HHInc \le 21,297$ 41 161				
$21,297 < HHInc \le 42,593$ 56 55					
$42,593 < HHInc \le 85,185$ 19 47					
HHInc > 85,185 10 46					
Categories of HHVeh					
HHVeh = 0	19	12			
HHVeh = 1 115 110					
HHVeh = 2	HHVeh = 2 161 329				
$HHVeh \ge 3$ 97 224					

- Search candidate TAZs: We search TAZs that a driver could reach within a time threshold. Specifically, for any daily activities, we set the lower bound and upper bound of arrival time. If the driver arrives at the centroid of a TAZ within the time-boundary, this TAZ falls into the candidate set. We empirically set 0.8t_{drive} and 1.2t_{drive} as the lower bound and upper bound, respectively, where t_{drive} is the driving time generated by Markov chain, which is formally defined as the number of continuous driving states multiplied by the time resolution of the Markov chain;
- Determine the exact destination TAZ: Once candidate TAZs are identified, we utilize historical OD distribution probability from the start TAZ to all candidate TAZs to determine which TAZ the trip arrives at. To achieve this, OD data for a typical workday is divided

- into four subsets time periods (i.e. 12:00 am 6:00 am, 6:00 am 12:00 pm, 12:00 pm 6:00 pm, and 6:00 pm 12:00 am). Trip counts from the source TAZ to candidate TAZs are fetched from one of the subsets depending on the activity start time. The probability that a trip arrives at any candidate TAZ is proportional to trip count from source TAZ to that TAZ divided by trip counts to all candidate TAZs. The OD data is split by time periods because many activities possess strong temporal patterns, such as work-based trips;
- Pinpoint trip destination: After the destination TAZ is determined, we randomly assign one POI with corresponding trip purpose as the activity destination in the determined TAZ. For instance, if the activity purpose is "dine-in", we choose one POI with the label "restaurant". The mapping between activity purpose and POI label can be found in Section 4.4 POI data.

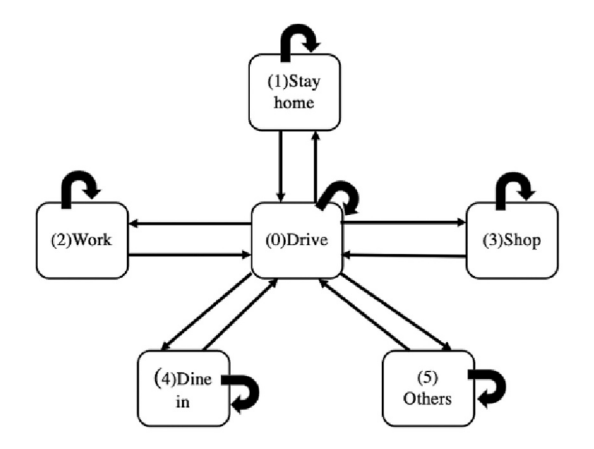
Since each daily activity could contain multiple intermediate stops, the location mapping process is iterated starting from home until the last activity is completed. Note that if location mapping fails to capture any intermediary stops for some reason (e.g. long driving duration), this activity would be discarded from the system.

4.4. EV assignment and energy consumption model

MATSim is used to simulate all vehicles' daily trips within a study region. As post-simulation analysis, we perform EV assignment and set up public charging rules to determine public charging demand distribution. For EV assignment, we apply the EV adoption probability model developed by Javid and Nejat (2017). Javid and Nejat (2017) developed a logit model using the California Statewide Travel Survey data and validated it against another dataset in Delaware, Texas. The result showed robust transferability in terms of the Area Under the Curve (AUC) - a classic metric for classification models. We therefore directly adopt the model here to assign EV drivers in the study region. The mathematical formulation is presented as follows:

$$p(x) = \frac{1}{1 + e^{-\left(\sum a_i * x_i + \beta\right)}}$$
 (1)

where x represents an individual that could potentially become an EV driver in a household, x_i denotes internal or external factor that influences the purchase decision of individual x, and α_i is the corresponding coefficient. p(x) is the estimated EV adoption probability for individual x. Eq. (1) is a logit model considering socioeconomic and demographic features. Table 3 lists the values of the variables and corresponding coefficients used. Individuals' attributes, including age, income, vehicle ownership, and household size, are used to calculate the



(a) Markov chain diagram of state transition

 $T_t = \begin{bmatrix} P_{00}^t & P_{01}^t & P_{02}^t & P_{03}^t & P_{04}^t & P_{05}^t \\ P_{10}^t & P_{11}^t & P_{12}^t & P_{13}^t & P_{14}^t & P_{15}^t \\ P_{20}^t & P_{21}^t & P_{22}^t & P_{23}^t & P_{24}^t & P_{25}^t \\ P_{30}^t & P_{31}^t & P_{32}^t & P_{33}^t & P_{34}^t & P_{35}^t \\ P_{40}^t & P_{41}^t & P_{42}^t & P_{43}^t & P_{44}^t & P_{45}^t \\ P_{50}^t & P_{51}^t & P_{52}^t & P_{53}^t & P_{54}^t & P_{55}^t \end{bmatrix}$

(b) Transition matrix at time t

Fig. 3. The Time-inhomogeneous Markov chain at time t.

Table 3 Variables and coefficients in EV adoption probability model.

Variable	Coefficient	Explanation	Constant
x_{age}	0.04	Driver's age	NA
x_{car_share}	0.911	Weather the vehicle is shared with other drivers	0.01
x_{trip_dur}	0.001	Average daily trip duration (miles)	52.4
x_{income_level}	0.461	Categorized variable indicating the level of	NA
		income with 1 denoting the lowest and 5	
		denoting the highest income	
$x_{household}$	-0.071	Categorized variable indicating the size of	NA
		household	
$x_{education}$	0.274	Categorized variable indicating the	4.76
		education level	
$x_{station_num}$	0.811	Charging station per capita	0.5
x_{gas_price}	2.8	The gas price (dollar/gal)	3.6
x_{elec_price}	0.077	The electricity price per (cent/kWh)	14.6
x_{veh_num}	-0.055	The number of vehicles owned by the driver	NA
β	-19.629	Constant term	NA

EV adoption probabilities. Variables with minor variations across regions or those that are difficult to obtain, such as gas price and education level, are set as constants for simplicity. Note that constant values (excluding x_{gas_price} and x_{elec_price}) and coefficients are referenced from (Javid & Nejat, 2017).

Public charging is a stochastic process. The majority of charging mechanisms are based on the state of charge (SoC) or equivalent range anxiety (Hu et al., 2018; Wang et al., 2014). In this study, two types of charging are considered - standard charging (Level 2) and fast charging (Level 3). SoC is updated for each trip once the driver arrives at the next destination. Charging behavior is determined by the current SoC and dwell time. A flowchart with explicit charging rules is presented in Fig. 4.

The proposed charging rules consider three charging behaviors: no charging, standard charging, and fast charging. According to Zou et al. (2016), over 75% EV drivers will not charge their vehicles unless SoC drops below 50%. For this reason, we assume EV drivers would consider public charging only when SoC is below 50%. When SoC drops below 50%, EV driver may conduct Level 2 charging. However, driver may refuse to charge if the dwell time D is too short. Hence, 30 min of minimal charging time is used to determine Level 2 charging preference (Yi & Bauer, 2016). However, if SoC drops below 15%, EV driver will opt for fast charging regardless of the dwell time.

Besides charging rules, initial SoC should be determined as well. In fact, not all EV drivers have access to home charging equipment, and overnight charging might not be necessarily performed. The assumption

of fully charged batteries before drivers depart home is not practical. Instead, the initial SoCs is generated from a normal distribution (Zheng, Wang, Men, Zhu, & Zhu, 2013). It is worthy to mention that the aforementioned charging rules only produce charging requests (or demands). It does not imply that charging is fulfilled at that moment, since public charging stations may or may not exist nearby for each charging request. The actual charging fulfillment will be discussed in optimization analyses.

4.5. CMCLP optimization model

We consider both standard charging and fast charging. Table 4 and Table 5 give the description of input parameters and decision variables for CMCLP model, separately. The objective of CMCLP is to maximize the coverage of public charging demands under a variety of constraints, including charging capacity, access distance, and investment budget. For charging capacity, it is applied by different hours-of-the-day to consider surging demands during peak hours. In order to formulate the hours-of-the-day constraints for charging stations, charging demands (i. e., charging request) are discretized. For instance, if a public charging event is performed between 8:00 AM and 10:45 AM, it will be first rounded to a 3-h request (from 8:00 AM – 11:00 AM), and discretized by hour - 8:00 AM-9:00 AM, 9:00 AM-10:00 AM, and 10:00 AM-11:00 AM. The charging demands is determined by the proposed charging rules in Fig. 4, while the energy consumption of each hourly demand (i.e., d_{it}^{L2} and d_{it}^{L3}) can be calculated based on the power of chargers and dwell time at the destination. As for accessibility, this study assumes that new public charging stations can only be installed at public parking lots due

Table 4 Description of input parameters.

Input parameters	Descriptions
i	the index of EVs that have daily charging requests
I	the set of EVs that have daily charging requests
j	the index of public parking lot location
\overline{J}	the set of public parking lots
t	the index of the hour of the day
T	the set of hours of the day
$d_{it}^{L2} \ d_{it}^{L3}$	the hourly L2 charging demand (kWh) of vehicle i at hour t
d_{it}^{L3}	the hourly L3 charging demand (kWh) of vehicle i at hour t
P	the total investment budget for public charging stations
P_{max}	the maximum number of ports for each charging station
C^S	the cost for installing a single charging station
C^{L2}	the equipment cost for one standard charging port
C^{L3}	the equipment cost for one fast charging port

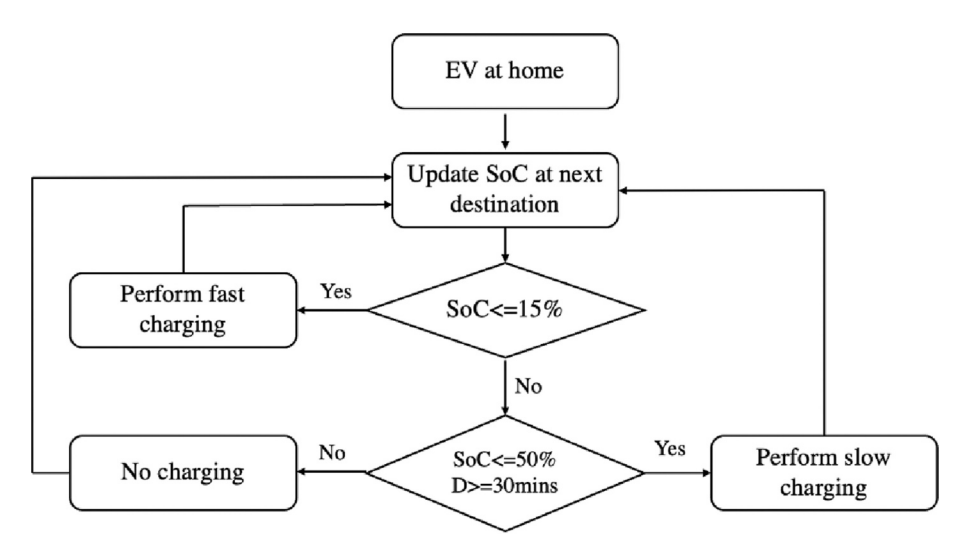


Fig. 4. Rules for EV charging.

Table 5Description of decision variables.

Decision variables	Descriptions
$y_j^{L2} \\ y_j^{L3}$	the number of L2 chargers installed at public parking lot j the number of L3 chargers installed at public parking lot j
z_{itj}^{L2}	$\left\{ \begin{array}{ll} 1 \;\; , \mbox{if} \; d_{it}^{\rm L2} \; \mbox{can be satisfied by the charging station at} \; j \; \mbox{and hour} \; t \\ 0 \;\;\; , \mbox{otherwise} \end{array} \right.$
z_{itj}^{L3}	$\left\{ \begin{array}{cc} 1 & \text{, if } d_{it}^{L3} \text{ can be satisfied by the charging station at } j \text{ and hour } t \\ & 0 & \text{, otherwise} \end{array} \right.$
x_i	\int 1 , if parking lot j is used for installing public charging station
Ω_j	$\left\{ \begin{array}{c} 1 & \text{, if parking lot } j \text{ is used for installing public charging station} \\ 0 & \text{, otherwise} \\ \text{the set of } (i,t) \text{ that can be served by the public parking lot } j \end{array} \right.$

to space and facility requirements, and a catchment area with a radius r is created for each public parking lot to quantify the accessibility of drivers to the parking lot. If the driver's current location falls within the catchment area, then the driver's current charging request is considered to have the potential to be fulfilled by that parking lot (where a charging station can be sited). The last constraint is the investment budget. It is calculated as the sum of assets values of existing charging stations, since we aim to optimally reallocate existing charging stations. The mathematical formulation of CMCLP is defined as follows:

Objective function:

$$Maximize \sum_{i \in I} \sum_{t \in T} d_{it}^{L2} \sum_{j \in J_i} z_{itj}^{L2} + \sum_{i \in I} \sum_{t \in T} d_{it}^{L3} \sum_{j \in J_i} z_{itj}^{L3}$$
(2)

Subject to:

$$y_j^{L2} + y_j^{L3} \le P_{max} X_j, \forall j \in J$$
 (3)

$$\sum_{i \in I} \left(C^{S} x_{j} + C^{L2} y_{j}^{L2} + C^{L3} y_{j}^{L3} \right) \le P \tag{4}$$

$$\sum_{(i,j)\in\Omega} z_{iij}^{L2} \le y_j^{L2}, \forall j \in J, \forall t \in T$$

$$\tag{5}$$

$$\sum_{(i,i)\in\Omega_i} z_{iij}^{L3} \le y_j^{L3}, \forall j \in J, \forall t \in T$$
(6)

$$x_i = \{0, 1\}, \forall k \in K \tag{7}$$

 $y_i^{L2} \in \mathbb{N}, \forall j \in J$

 $y_i^{L3} \in \mathbb{N}, \forall j \in J$

 $z_{ii}^{L2} = \{0, 1\}, \forall i \in I, \forall t \in T, \forall j \in J$

$$z_{iii}^{L3} = \{0, 1\}, \forall j \in I, \forall t \in T, \forall j \in J$$

The objective function (2) maximizes the total service of hourly Level 2 and Level 3 charging demands. Constraints (3) guarantee that the total number of standard and fast charging ports should be no more than P_{max} if charging station is sited at public parking lot j. Constraint (4) imposes the total budget limit for installing public charging stations and ports. Constraints (5) and (6) set the hourly capacity for L2 and L3 chargers, separately. For each charging station x_j , the number of standard/fast hourly demands it covers at each particular hour t should be less than the total number of standard/fast charging ports $(y_j^{1,2}/y_j^{1,3})$. Constraints (7) impose integer or binary integer restrictions on decision variables.

5. Result and analysis

5.1. Case study

The Salt Lake City (SLC) metropolitan area is used as a case study to

demonstrate the framework implementation. SLC metropolitan region covers approximately 940 km² and includes 407,442 households with about 826,000 vehicles. The entire study area consists of 1090 TAZs. A report from American Driving Survey (Triplett, Santos, Rosenbloom, & Tefft, 2016) indicates that 78% of drivers perform at least one driving trip in a day on average. Therefore, it is assumed that 644,300 vehicles will be on the road for simulation. In MATSim, a day trip is defined as a round trip starting from home and returning home before midnight. Besides, a day trip can include several intermediate stops (e.g., workplaces, restaurants, etc.) After data processing, 17.4% of trips after location mapping are considered invalid and therefore discarded. The final inputs to MATSim thus contain 532,460 trips. MATSim takes these planned trips as inputs, and optimizes driving events iteratively based on co-evolutionary principle. In this study, MATSim is executed with 100 iterations. When the iteration time reaches 55, the computation is nearly converged. For post-MATSim analysis, road traffic is assumed to consist of light-duty vehicles and EVs. EV adopters are determined by Eq. (1). The required socioeconomic variables in Eq. (1) for each synthetic driver is known, thus its probability in adopting EV can be calculated. The EV adoption probabilities across TAZs (Fig. 5) range from 0.6% to 21% with mean value of 4.3%. Correspondingly, among the 532,460 drivers, 22,737 drivers are assigned with EVs. EV charging profile is implemented using the rule specified in Section 3.4. EV Assignment and Energy Consumption Model. The initial SoC is empirically determined by a normal distribution with $\mu = 0.85$ and $\sigma = 0.3$, considering that home charging accounts for over 80% of all charging events (Smart & Schey, 2012). As for other EV parameters, EVs' battery capacity can be varied widely from 17.6 to 100 kWh depending on the manufacturers and car models. For simplicity, the battery capacity is consistently assumed as 62 kWh (Nissan Leaf S Plus). A fixed energy consumption rate is assumed as 0.3 kWh/mile (Plugin America, 2016).

5.2. Stochastic daily activities from Markov chain

Stochastic activities for both light-duty vehicles and EVs are generated from time-inhomogeneous Markov chain, trained using ATUS data. Note that the ATUS data is extracted only for weekdays, since weekends have significantly different activity patterns. The distribution of the proposed six activity states at each time step of a day is displayed in

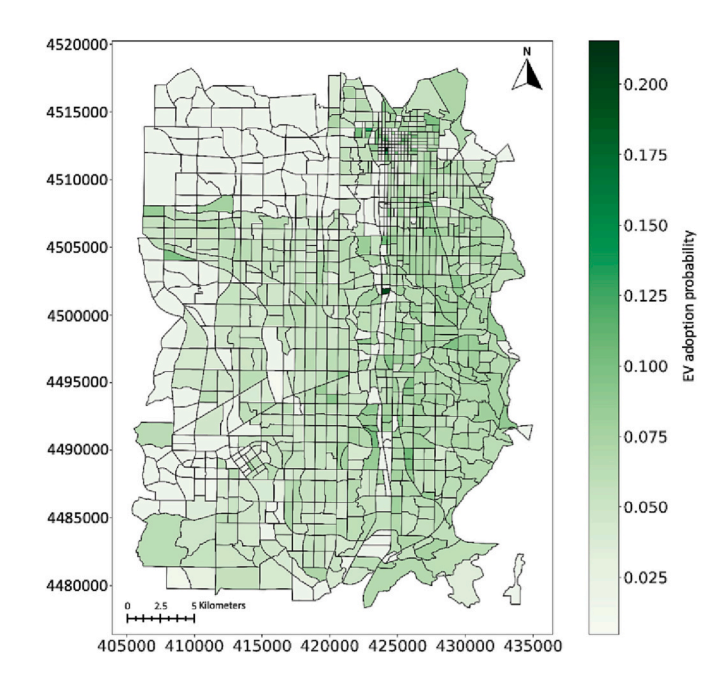


Fig. 5. The EV adoption probability distribution in SLC metropolitan area. The map is projected and displayed in UTM Zone 12 N, with the coordinates' units in meters.

Fig. 6. Moreover, activity distribution from ATUS is included for comparison.

In Fig. 6, it is found that daily activity distribution from synthetic drivers generated by the Markov chain follows a similar pattern as the real-world distribution. During the daytime, majority of drivers park their vehicles at workplaces. Apart from work, many drivers also conduct other activities, such as shopping, dining, or entertaining during the daytime. Several existing studies limit activities for EV users with only staying home, driving, and working states. As seen from Fig. 6, such oversimplification can induce biased results by overlooking the impact from nonwork-related activities to public charging. It is also observed that two peaks of traffic flow occur around 8:00 AM and 6:00 PM, respectively. Overall, the simulated daily activities distribution conforms to the reality.

In the next step, daily activities from synthetic drivers are fed into MATSim to perform agent-based simulation onto the road network. MATSim is used to model activities in a single day for agents (i.e., drivers) based on the co-evolutionary principle. During iterations, a certain portion of drivers' plans, such as route and departure time, will be modified to search for optimal choices until the entire system reaches equilibrium state. The optimized events for those agents from MATSim can be used as important basis for post-analyses, such as public charging behavior modeling. We first explore the spatial distribution of activities from the MATSim output. Specifically, trip destination count is aggregated by TAZ and compared with real-world historical trip observations as shown in Fig. 7.

Note that the stochastic daily activity generated by the Markov chain does not contain any geolocation information. Location mapping technique is performed to remedy this. The location mapping process fully

utilizes POI, road network, and OD information to match the trips within the study region. All trip destinations, including intermediary stops, are aggregated by TAZ in Fig. 7(a). It is found that the distribution of synthetic trips appears to be quite similar to the actual trip distribution. Most daily activities are concentrated in northern part of the study region. The downtown area represents dense trip destinations as well, yet the color in those TAZs is relatively light. This is due to the smaller area size of the TAZs within downtown. Note that the total number of actual trip destinations is 2,681,140, while the number of synthetic trip destinations is 2,093,401. Such discrepancy is likely attributable to the filtered 17.4% trips in MATSim.

The temporal and spatial analyses sufficiently demonstrate that the simulated daily activities are similar to real-world situations. In the next step, analyses related to public charging behaviors are performed to validate against real-world public charging observations.

5.3. Real-world public charging validation

MATSim outputs the optimized driving behaviors on a daily basis. Based on the MATSim outputs, EV assignment and charging demand generation are performed as postsimulation offline analysis. The assigned 22,737 EV drivers generated 1586 charging requests during a day, with 1366 events belonging to standard charging requests. In order to compare the estimated public charging demand with real-world observations, the energy data crawled from ChargePoint is averaged by day. Fig. 8 presents the spatial distribution of estimated public charging demand and actual energy consumption, where the green dots represent public charging stations, and a larger radius indicates higher energy consumption in reality. The background layer shows aggregated

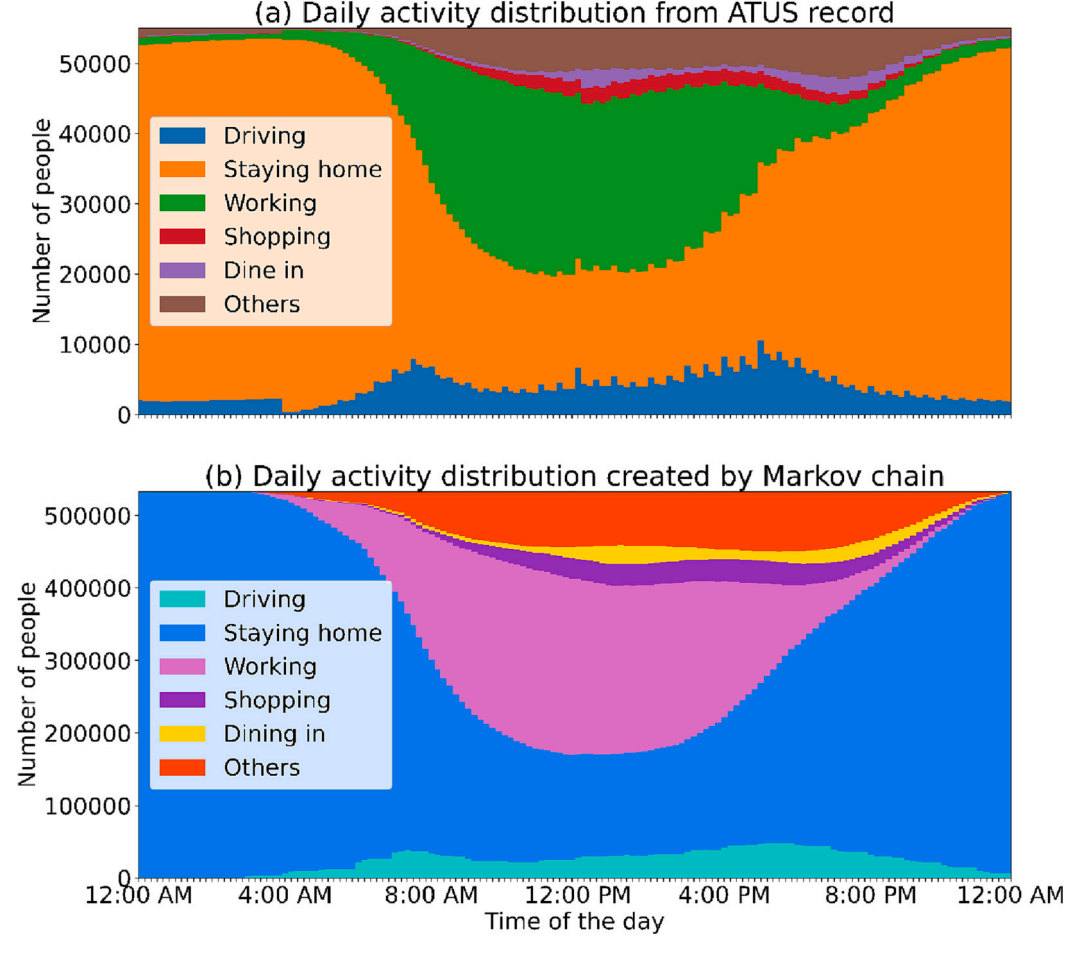


Fig. 6. A weekday's activity distribution from (a) real-world data; (b) time-inhomogeneous Markov chain.

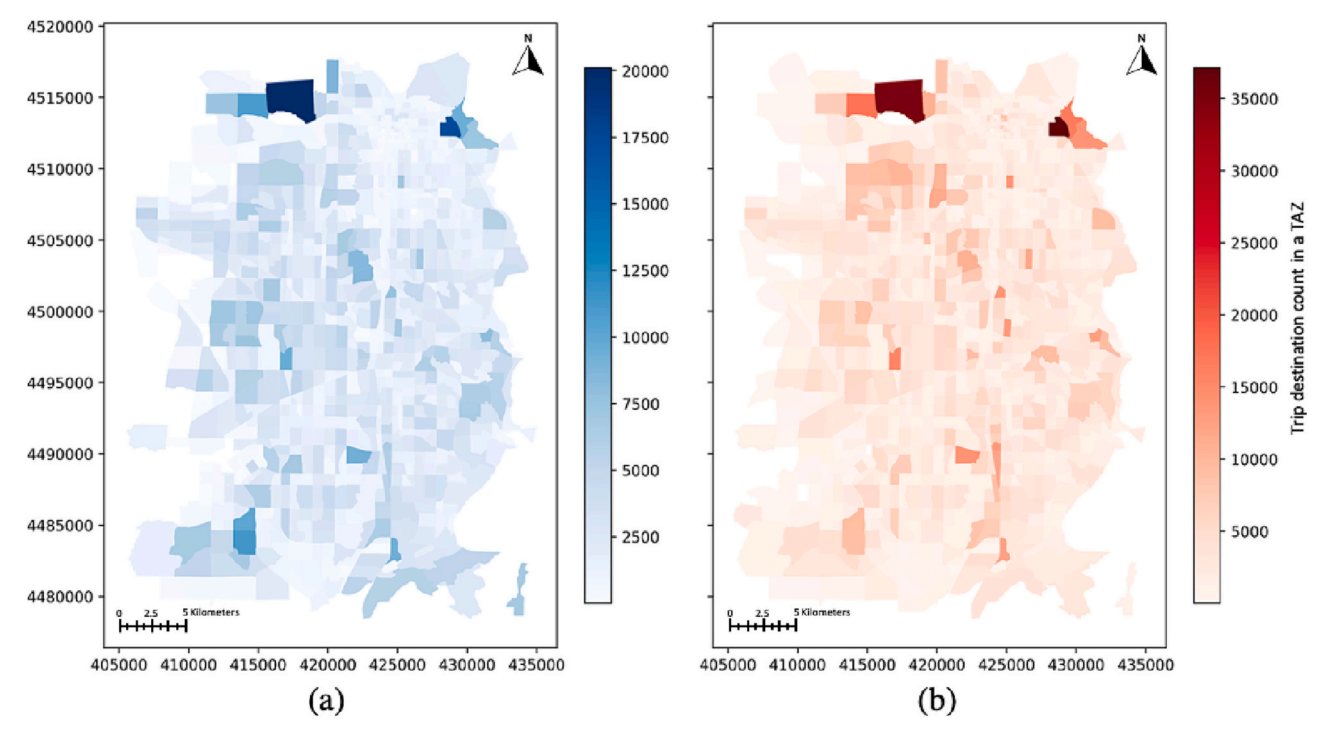


Fig. 7. The spatial distribution of trip destination: (a) trip destination from simulation and (b) trip destination from real-world data on a typical weekday. The map is projected and displayed in UTM Zone 12 N, with the coordinates' units in meters.

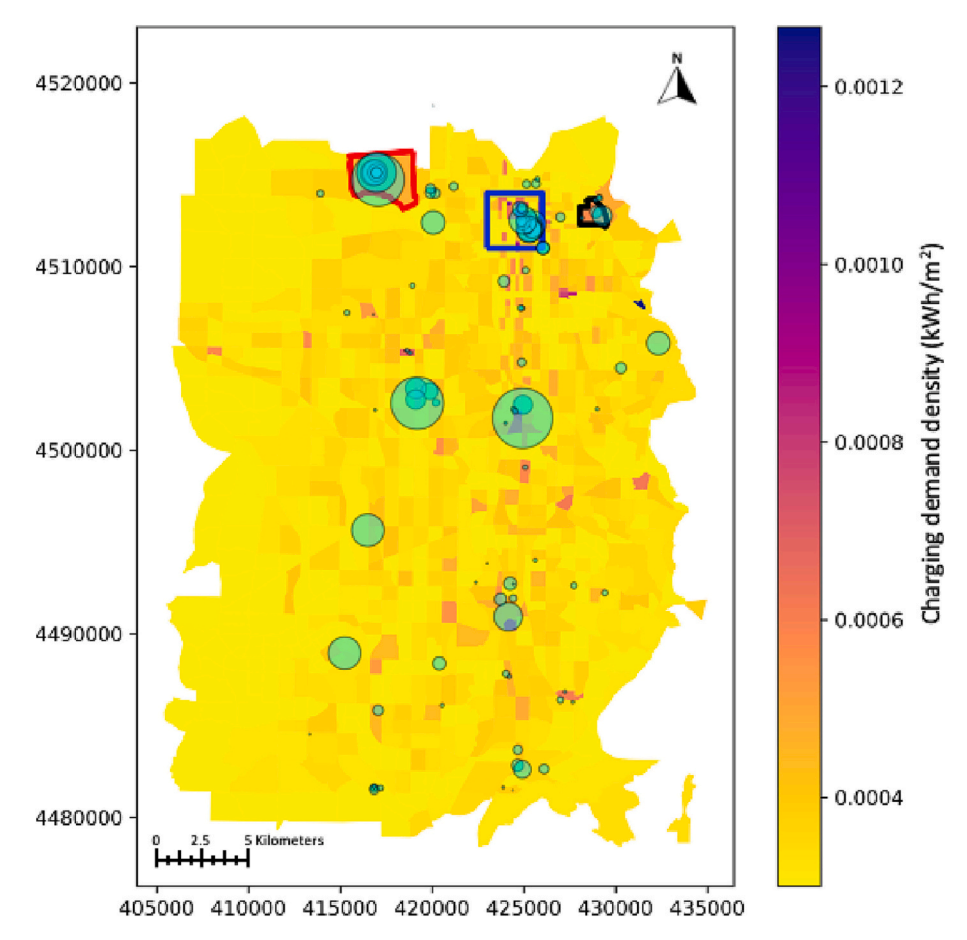


Fig. 8. Spatial distribution of real-world public charging energy consumption (green circle) and estimated charging demand density by TAZ (background layer). The map is projected and displayed in UTM Zone 12 N, with the coordinates' units in meters. (For interpretation of the references to color in this figure legend, the reader is referred to the web version of this article.)

estimated charging demand by TAZ with the color representing charging demand density, defined as the summed daily energy request divided by the area of TAZ (kWh/ m^2). In general, it is observed that public charging stations in TAZs with higher estimated charging demand density tend to have higher energy consumption. For instance, SLC downtown (highlighted by blue square) demonstrates both higher public charging demand density and energy consumption. That is likely because TAZs in the downtown area have dense trip destinations and are sited with a large amount of POIs related to working, entertaining, and other purposes. Note that the charging stations around the airport (highlighted by

red polygon) indicate high usage frequency, while charging demand density is relatively low. This is due to the large area size for that TAZ. On the contrary, TAZs in South Salt Lake County have relatively lower charging demand density due to fewer trip destinations as shown in Fig. 7. We also notice that several TAZs with high estimated public charging demand density are not currently allocated with public charging stations. The proposed charging station location optimization can effectively address this issue. Apart from spatial distribution, temporal trends for public charging station utilization are worthy of exploration. To this end, we select three TAZs with different levels of

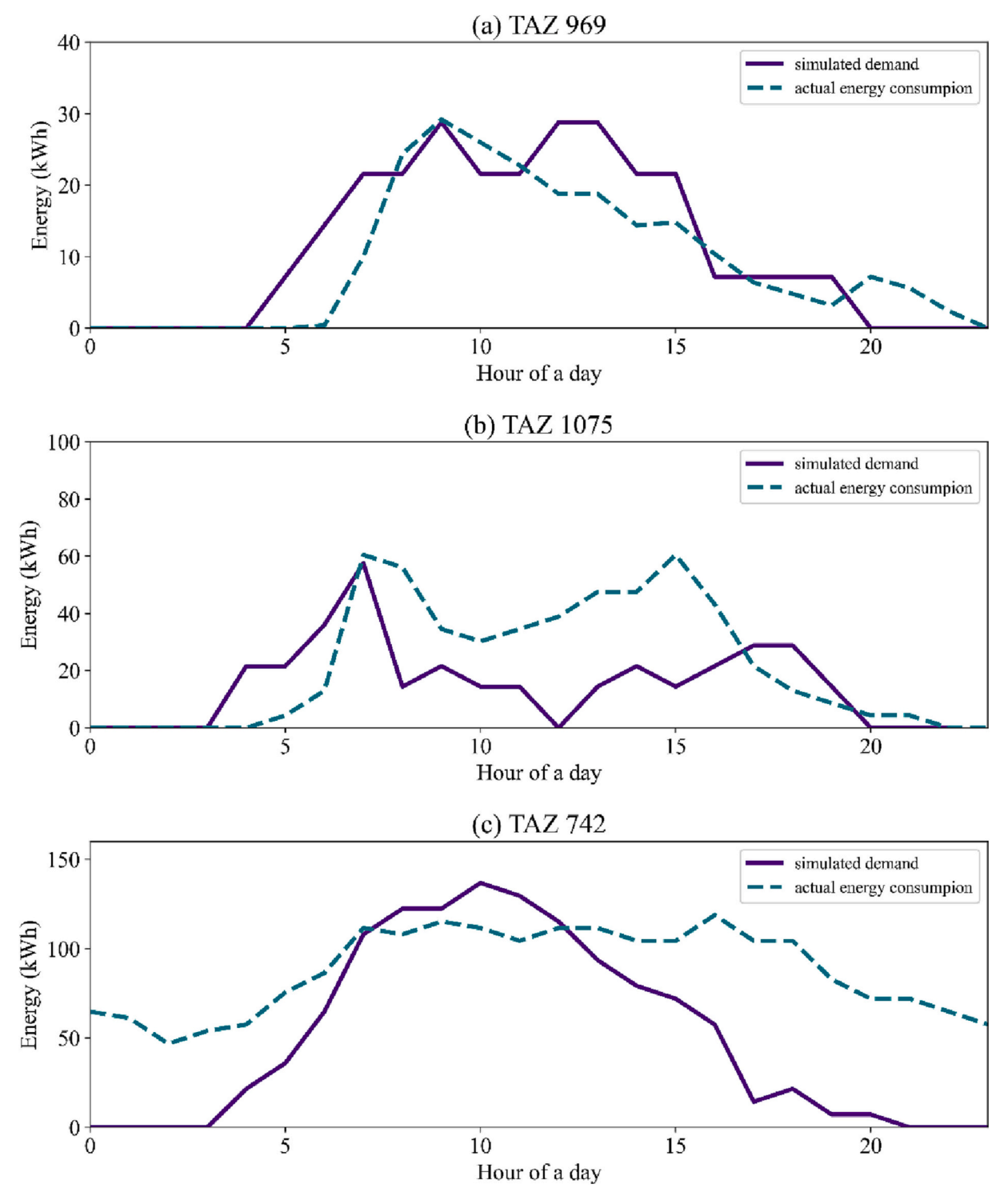


Fig. 9. Real public charging energy consumption versus simulated public charging demand in representative TAZs.

energy demand, and compare the estimated daily charging demand at different times-of-the-day with real-world charging station utilization records. The results are presented in Fig. 9.

Fig. 9 compares estimated energy demand and actual energy consumption at the TAZ level in areas that have varying land-use patterns. TAZ 969 is a small block located in SLC downtown. The public charging peaks at around 9:00 AM, and the demand gradually decreases afterwards. Such charging pattern is generally found in regions with lots of office buildings. Fig. 9(b) shows the charging pattern of TAZ 1075, an area in the vicinity of downtown (highlighted by black in Fig. 8). Although office buildings are not densely located in this TAZ, the University of Utah and University hospital are located in within, serving as major traffic generator. However, the charging pattern is different from that in the downtown area, where two peaks (one around 8:00 AM and one around 3:00 PM for public charging) are found. This can be explained by the fact that some EV drivers did not come to the location for work. Instead, drivers could be students or patients conducting different activities other than work. Lastly, TAZ 742 (highlighted by red in Fig. 8) includes the SLC international airport. Due to the uniqueness of airport, trip density and public charging demand are significantly higher than other TAZs as indicated in Fig. 9(c). Another distinction for this TAZ is that many EVs are left charging overnight at the airport. However, when estimating the charging demand in our framework, we only consider the potential charging opportunities that are linked between two activities via driving during the day (e.g., home, work, shopping, etc.) Yet overnight charging is neither modeled nor within the scope of our study. Overall, the daily charging pattern matches the actual energy consumption for those selected TAZs without large deviation during the

While the majority of TAZs show consistent pattern between the estimated charging demand and actual energy consumption, there are several locations with high estimated charging demand density yet have not been assigned any charging station, and locations with charging stations that are significantly underutilized. Another potential problem is that with the increase in EV adoption, public charging demand would increase significantly, which poses challenges to existing charging stations especially during peak hours in popular regions. For this reason, charging stations should be optimally reallocated such that they can be effectively utilized while avoiding extremely long queues during peak hours in the future. In the following section, we focus on optimizing charging stations considering demand increases in the future.

5.4. Public charging station optimization result

The CMCLP model aims to maximize the coverage of the public charging demand considering charging capacity, access distance, and investment cost. As for the access distance, EV drivers may opt for alternative solutions such as home charging if walking distance is beyond 0.91 km according to (Seneviratne, 1985). For this reason, radius *r* for the catchment area for each public parking lot is set as 1000 m. Meanwhile, the investment budget is calculated using the current 109 charging stations with 516 Level 2 ports. In general, the cost of installing a charging station is approximately \$5500 including labor cost and materials, and the average prices for L2 port and L3 port are around \$2500 and \$5500, separately (Borlaug, Salisbury, Gerdes, & Muratori, 2020). The total budget is therefore approximated at \$1.89 million (\$5500*109 + \$2500*516). For parameters related to charging stations, Level 2 chargers are uniformly assumed as J1772 plugs with power of 7.2 kW, and Level 3 chargers are uniformly assumed as CHAdeMO plugs with power of 50 kW. The maximum number of ports P_{max} is set as 8 for simplicity.

In this study, we optimize charging station locations considering charging demand increase in the future. The main purpose of considering demand increase is to handle exponential EV adoption increase. Besides, providing insightful guidance for new charging station deployment in the future is of practical use to local agencies to assist

with infrastructure planning and decision making. A report from Bloomberg projects that the national EV adoption would reach 12% in 2030 and >50% in 2050 (Ghamami, Zockaie, Wang, & Miller, 2019). Given such projection, scaling factor 3.5 is used to augment EV penetration from 4.3% to 15% as charging demand increases. Subsequently, we estimated such public charging demand according to the designed energy consumption model and charging rules. Upon scaling, 80,182 EVs with 5820 daily public charging events are identified in SLC metropolitan area. 5061 are slow charging events and 759 are fast charging events. Here, the CMLCP is solved using a commercial optimization solver Gurobi. Optimized layout is displayed in Fig. 10.

The orange triangles in Fig. 10(a) and (b) denote estimated public charging demand. The black dots in Fig. 10(b) represent available public parking lots that can be used to build charging stations. The magenta circles in Fig. 10(a) and green circles in Fig. 10(b) are current and optimized charging stations respectively with a radius representing the number of chargers. After optimization, the original 109 charging stations (516 Level 2 ports) are transformed to 64 charging stations with 313 Level 2 ports and 136 Level 3 ports reallocated throughout the region. Although fast charging demands only account for 13% of total demands, 30% chargers are Level 3 after optimization. Level 3 charging can provide full miles of range within an hour, which satisfy public charging need in a shorter time when drivers conduct short-duration activities other than work. It is observed that public charging stations are densely congregated in SLC downtown area both before and after optimization due to the large amount of public charging demand. Overall, public charging stations are mostly reallocated in the northern part of SLC metropolitan area after optimization, most likely due to the concentration of outdoor activities. Besides, southern area has fewer public parking lots that allow for new charging stations siting. One issue with the optimization is that several spots with significant charging demands are not assigned with charging stations, such as the airport. That is due to the unavailability of public parking lots. However, commercial buildings can possibly be used to build charging stations to replace public parking lots for future deployment.

The CMCLP solution presents an optimized reallocated charging station layout. Yet, in practice, future EVSE deployment should be considered upon existing charging stations. As such, we evaluate the overall utilization between existing charging stations and optimized stations. Specifically, we split existing charging stations into two groups - charging stations that are overlapped with optimized charging stations (group 1) and charging stations that are not overlapped with optimized charging stations (group 2). For optimized results, we also split them into two groups - charging stations that are overlapped with existing charging stations (group 3) and charging stations that should be newly installed (group 4). For groups 1 and 3, overlapping is defined as the distance between two stations being <1 km. To observe the utilization efficiency for each group of charging stations, we assign each charging request to the nearest station within the walk distance (1 km) and aggregate the number of charging requests by maximum, mean, and minimum. The charging requests assignment are performed for existing layout and optimized layout, separately. Table 6 shows the basic charging station information and the utilization status for each group.

In Table 6, it is observed that the optimized layout has a higher coverage rate than existing charging stations. Specifically, group 2 presents extremely low coverage with 15.5 times per day on average. Existing charging stations in group 2 are mostly distributed in remote areas or in the vicinity of dense clusters. One practical guidance for future EVSE installation is to keep maintaining those overlapped charging stations (group 1) and moderately adjust the number and type of charging ports. For those underutilized charging stations (group 2), we should reallocate them to new areas to fulfill higher (or new) charging demands.

In order to validate that the optimized public charging stations layout could provide more effective charging utilization, UrbanEV-Contrib is applied to simulate public charging behavior in MATSim.

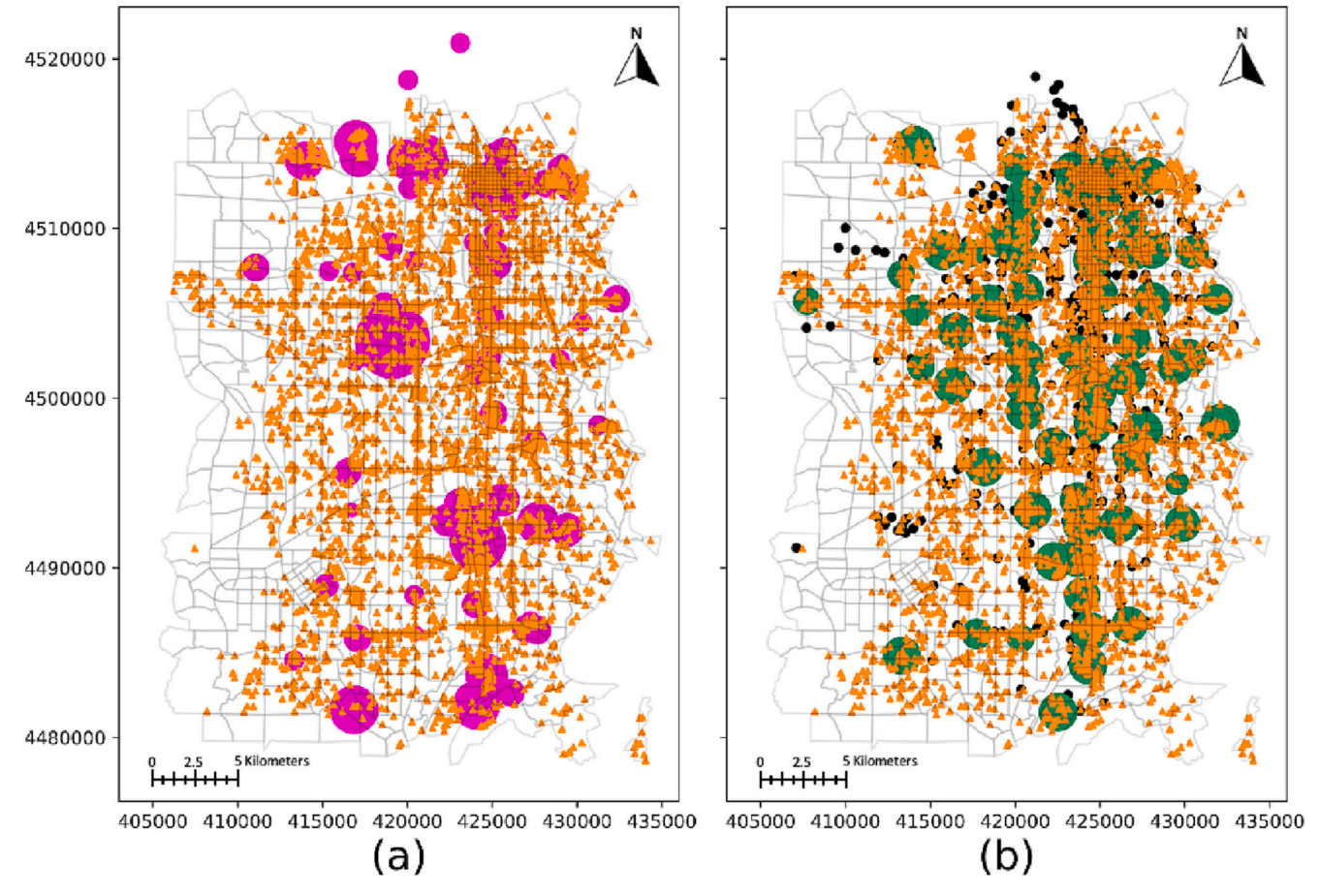


Fig. 10. Public charging demand distribution and (a) existing layout of public charging stations; (b) optimized layout of public charging stations. The map is projected and displayed in UTM Zone 12 N, with the coordinates' units in meters.

Table 6Utilization comparison between existing stations and optimized stations.

	Existing layout		Optimized layout	
	Group 1	Group 2	Group 3	Group 4
Station count	30	79	30	34
Port count	112	404	213	236
Slow charging port	112	404	151	162
Fast charging port	NA	NA	62	74
Min. requests covered	21	0	23	20
Avg. requests covered	45.0	15.5	46.8	40.7
Max. requests covered	110	59	120	72

UrbanEV-Contrib is an open-source framework capable of performing high-resolution analysis of urban electric mobility based on MATSim serve as a MATSim plug-in module (Adenaw & Lienkamp, 2021). By inputting charging configurations and rules, UrbanEV-Contrib returns charging states and events in time series, which serves as a sandbox validating charging infrastructure design on the city-scale. To compare charging effectiveness, MATSim is reperformed with scaled EV drivers and corresponding public charging requests. Existing charging stations and optimized charging stations are inserted into the simulation environment separately to satisfy those charging requests using UrbanEV-Contrib plug-in. The remaining SoCs is one important metric to reflect the effectiveness of public charging station deployment, since a high level of SoC values after completing a series of daily activities denotes that charging station locations can be easily accessed by EV drivers while they conduct other activities. For this reason, remaining SoCs are examined upon completion of people's daily activities under two different scenarios in Fig. 11.

The first column in Fig. 11 denotes drivers who consumed all EV energy after completing a series of daily activities. While it is not realistic to exhaust SoC entirely, it is an important metric to evaluate how many drivers failed to access public charging stations during their daily activities. Overall, the number of drivers with 0 SoCs by the end of the day decreased by 20% as a result of charging station optimization. When SoC is too low, drivers may have range anxiety. The optimized layout effectively decreased the number of drivers with low SoC values to ensure higher accessibility and reduce range anxiety. It is also noted that the number of drivers with high SoC values increased to some extent. Higher values of SoC at the end of the day indicate that optimized charging stations make longer trips feasible for more EV drivers. In the next step, we explore the temporal profile of charging station occupancy. The number of chargers in use at different hours-of-the-day are plotted in Fig. 12.

Fig. 12 shows a temporal shift of charger occupancy peak in the optimized scenario. One possible explanation is that charging stations are easier to be accessed after optimization. It is observed that the number of charging ports that are occupied during the day (8:00 AM to 3:00 PM) becomes less upon optimization. This is due to the fact of more Level 3 charging stations, enabling drivers to charge with a shorter time. With current layout of charging stations, the average charging time is 2.8 h, while the charging time is reduced to 2.5 h on average after optimization. Moreover, the optimized layout allows EV drivers to access charging stations with shorter walking distances. The average walking distance is reduced from 310 m to 270 m, providing drivers with more convenience.

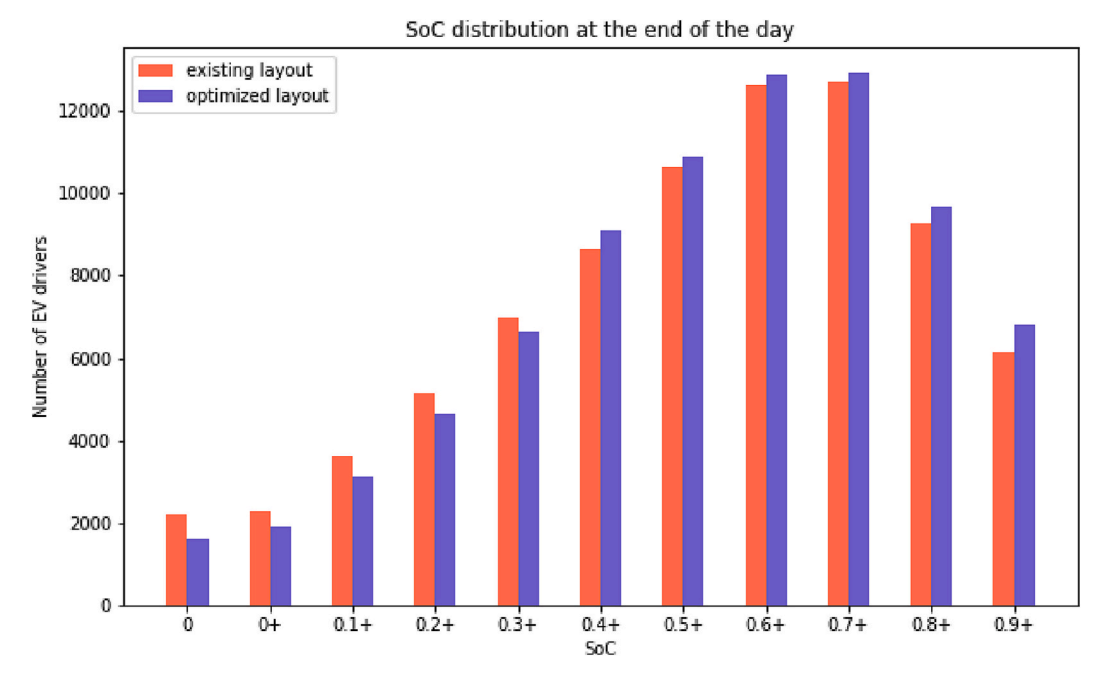


Fig. 11. SoC distribution after daily stochastic activities.

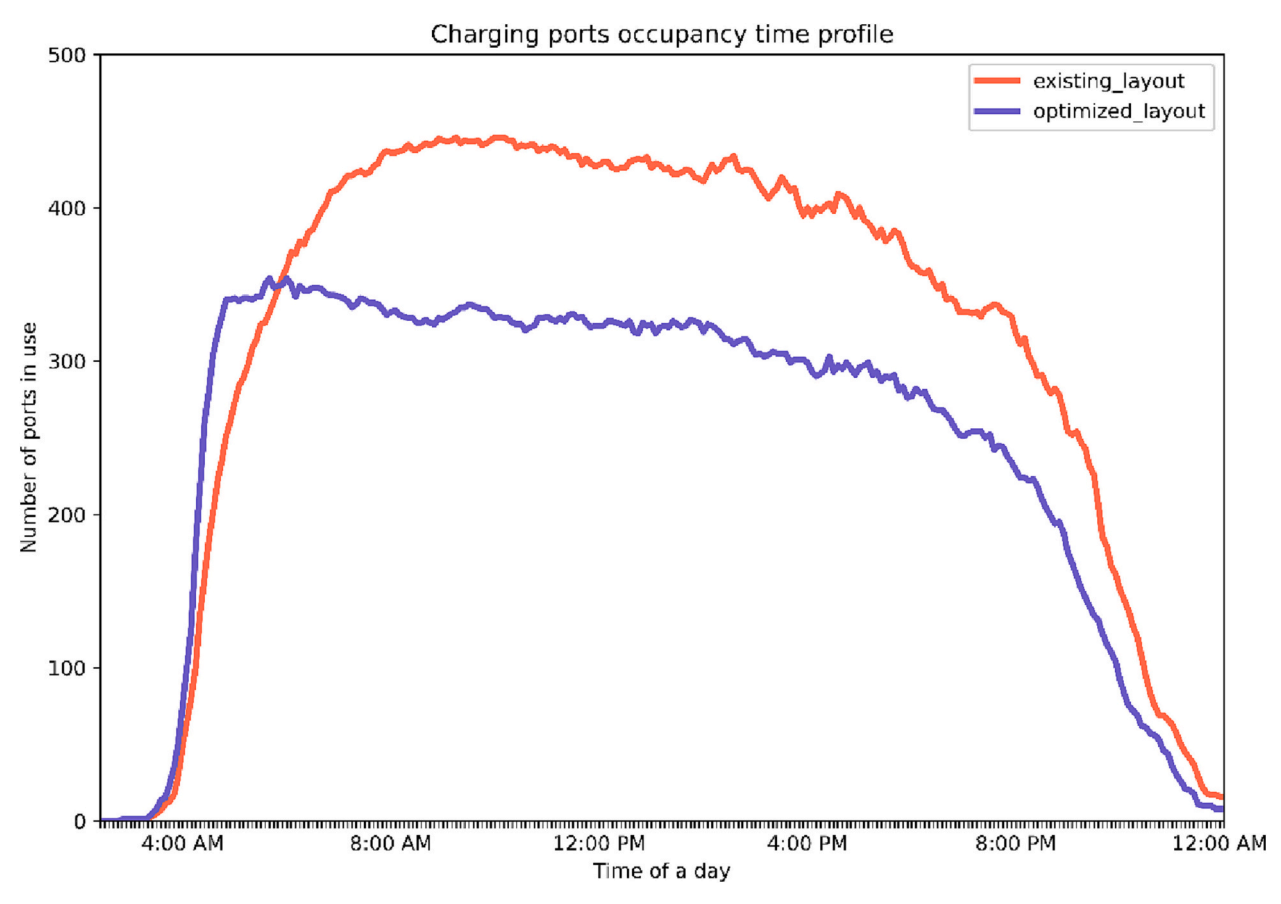


Fig. 12. The time profile of charger occupancy.

6. Conclusion

This paper presents an urban-scale public charging station location optimization framework through microscopic modeling. The modeling process follows the classical two-step approach (i.e. public charging

demand simulation and charging station location optimization). One major highlight is that the presented methodology addressed the oversimplification and limitations constrained in previous literature by utilizing high-fidelity city-scale road network, incorporating drivers' nonwork-based activities, and applying real-world EV distribution to develop a charging demand estimation model. Also, most existing studies failed to validate their proposed models due to the difficulty of retrieving real-world charging event records. As such, another novelty of this paper is the availability of real-work public charging events, which proved the validity of our modeling results. On top of the reliable simulation, we performed the CMCLP model to reallocate existing charging stations with the objective of maximizing the coverage of charging demand. The optimization model incorporates practical constraints such as walking accessibility and different charging modes. The optimized deployment scheme could provide meaningful guidance for Salt Lake City metropolitan areas and many alike.

We implement our methodological pipeline onto Salt Lake City metropolitan area to showcase the effectiveness. A series of validations are conducted to justify the robustness of simulation results. Specifically, the temporal and spatial distributions of drivers' daily activities are validated against ATUS data and historical OD data, respectively. Numerical results show that the time-inhomogeneous Markov chain with the proposed location mapping technique can be effectively used for trip generation, which is highly generalizable and replicable to other regions. Moreover, real-world public charging records are used to validate the spatiotemporal distribution of the synthetic public charging demands. It is found that the majority of TAZs demonstrate consistent pattern between the estimated charging demand and actual energy consumption. Once the fidelity of simulation results is guaranteed, we apply CMCLP optimization model with 15% EV penetration rate to account for the potential charging demand increase in the future. We further incorporate the plug-in UrbanEV-Contrib to perform agent-based simulation under the public charging context. It is found that the optimized layout can improve overall charging performance by decreasing the number of drivers with 0 SoCs by the end of the day over 20% and reducing the average charging time from 2.8 h to 2.5 h. The simulation experimental results offer meaningful political implications for governmental agencies. First, the existing coverage of fast charging stations in SLC metropolitan area is highly insufficient. Although the financial constraint is a major concern for building Level 3 chargers, agencies should still incentivize the fast-charging station deployment, since it is a critical step moving toward accelerated EV adoption and reaching net-zero emission goal by 2050. Second, low utility efficiency is identified at a lot of existing charging stations with extremely large number of ports and/or clustered densely in close vicinity. Instead, a decentralized design can effectively augment EV drivers' accessibility to the nearest charging stations. Lastly, some atypical activities could also impact public charging demand. Places such as airport and stadium are examples of locations where large charging demand could exist due to atypical activities.

This study is confined to investigating intracity travels (i.e. trips within the city) and intercity travels (i.e. trips that traverse multiple cities) are not within the scope. For those distant trips, EV drivers are more subject to range anxiety. Deploying fast chargers by identifying critical links or connection points for long-distance travels is worthy of exploration for future study.

CRediT authorship contribution statement

Zhiyan Yi: Conceptualization, Methodology, Formal analysis, Investigation, Data curation, Writing – original draft, Visualization. Bingkun Chen: Validation, Formal analysis, Investigation, Writing – review & editing, Visualization. Xiaoyue Cathy Liu: Conceptualization, Methodology, Data curation, Writing – review & editing, Supervision, Project administration, Funding acquisition. Ran Wei: Methodology, Resources, Writing – review & editing. Jianli Chen: Methodology, Resources, Data curation. Zhuo Chen: Validation, Resources.

Data availability

Data will be made available on request.

Acknowledgements

This article is based upon work partially supported by the National Science Foundation under Grant No. 2051226, and partially supported by the Mountain-Plains Consortium (MPC) of the U.S. Department of Transportation University Transportation Center (MPC-697). Any opinions, findings, conclusions or recommendations expressed in this material are those of the author(s).

References

- Adenaw, L., & Lienkamp, M. (2021). Multi-criteria, co-evolutionary charging behavior: An agent-based simulation of urban electromobility. World Electric Vehicle Journal, 12(1), 1–26. https://doi.org/10.3390/wevj12010018
- Asamer, J., Reinthaler, M., Ruthmair, M., Straub, M., & Puchinger, J. (2016). Optimizing charging station locations for urban taxi providers. *Transportation Research Part A: Policy and Practice*, 85, 233–246. https://doi.org/10.1016/j.tra.2016.01.014
- Axhausen, W., Horni, A., & Nagel, K. (2016). The multi-agent transport simulation MATSim.

 Ubiquity Press.
- Boeing, G. (2017). OSMnx: New methods for acquiring, constructing, analyzing, and visualizing complex street networks. Computers, Environment and Urban Systems, 65, 126–139. https://doi.org/10.1016/j.compenvurbsys.2017.05.004
- Borén, S., Nurhadi, L., Ny, H., Robert, K. H., Broman, G., & Trygg, L. (2017). A strategic approach to sustainable transport system development - part 2: The case of a vision for electric vehicle systems in Southeast Sweden. *Journal of Cleaner Production*, 140, 62–71. https://doi.org/10.1016/j.jclepro.2016.02.055
- Borlaug, B., Salisbury, S., Gerdes, M., & Muratori, M. (2020). Levelized cost of charging electric vehicles in the United States. *Joule*, 4(7), 1470–1485. https://doi.org/ 10.1016/j.joule.2020.05.013
- Charge Point. (2021). https://na.chargepoint.com/charge_point.
- Church, R., & ReVelle, C. (1974). The maximal covering location problem. Papers of the Regional Science Association, 32(1), 101–118.
- Deb, S., Kalita, K., & Mahanta, P. (2018). Impact of electric vehicle charging stations on reliability of distribution network. In Proceedings of 2017 IEEE international conference on technological advancements in power and energy: Exploring energy solutions for an intelligent power grid, TAP energy 2017, 1 (pp. 1–6). https://doi.org/ 10.1109/TAPENERGY.2017.8397272
- Deb, S., Tammi, K., Kalita, K., & Mahanta, P. (2018). Review of recent trends in charging infrastructure planning for electric vehicles. Wiley Interdisciplinary Reviews: Energy and Environment, 7(6), 1–26. https://doi.org/10.1002/wene.306
- Debnath, R., Bardhan, R., Reiner, D. M., & Miller, J. R. (2021). Political, economic, social, technological, legal and environmental dimensions of electric vehicle adoption in the United States: A social-media interaction analysis. *Renewable and Sustainable Energy Reviews*, 152(September), Article 111707. https://doi.org/10.1016/j.rser.2021.111707
- Dong, G., Ma, J., Wei, R., & Haycox, J. (2019). Electric vehicle charging point placement optimisation by exploiting spatial statistics and maximal coverage location models. *Transportation Research Part D: Transport and Environment, 67*(November 2018), 77–88. https://doi.org/10.1016/j.trd.2018.11.005
- Ghamami, M., Zockaie, A., Wang, J., & Miller, S. (2019). Electric vehicle charger placement optimization in Michigan: Phase I-highways (supplement I: Full tourism analysis). March https://www.michigan.gov/documents/energy/Tourism-Supplem entaryReport_662002_7.pdf.
- Google Place API. (2021). https://developers.google.com/maps/documentation/places/ web-service/search.
- Hakimi, S. L. (1964). Optimum locations of switching centers and the absolute centers and medians of a graph. *Operations Research*, 12(3), 450–459.
- He, F., Yin, Y., & Zhou, J. (2015). Deploying public charging stations for electric vehicles on urban road networks. Transportation Research Part C: Emerging Technologies, 60, 227–240. https://doi.org/10.1016/j.trc.2015.08.018
- Herberz, M., Hahnel, U. J. J., & Brosch, T. (2022). Counteracting electric vehicle range concern with a scalable behavioural intervention. *Nature Energy*, 1–8.
- Hodgson, M. J. (1990). A flow-capturing location-allocation model. Geographical Analysis, 22(3), 270–279.
- Hu, L., Dong, J., Lin, Z., & Yang, J. (2018). Analyzing battery electric vehicle feasibility from taxi travel patterns: The case study of new York City, USA. *Transportation Research Part C: Emerging Technologies*, 87(April 2017), 91–104. https://doi.org/ 10.1016/i.trc.2017.12.017
- Huang, K., Kanaroglou, P., & Zhang, X. (2016). The design of electric vehicle charging network. Transportation Research Part D: Transport and Environment, 49, 1–17. https://doi.org/10.1016/j.trd.2016.08.028
- Javid, R. J., & Nejat, A. (2017). A comprehensive model of regional electric vehicle adoption and penetration. *Transport Policy*, 54(November 2016), 30–42. https://doi. org/10.1016/j.tranpol.2016.11.003
- Khan, S. U., Mehmood, K. K., Haider, Z. M., Rafique, M. K., & Kim, C. H. (2018). A bilevel EV aggregator coordination scheme for load variance minimization with renewable energy penetration adaptability. *Energies*, 11(10). https://doi.org/10.3390/en11102809
- Kontou, E., Liu, C., Xie, F., Wu, X., & Lin, Z. (2019). Understanding the linkage between electric vehicle charging network coverage and charging opportunity using GPS travel data. *Transportation Research Part C: Emerging Technologies*, 98(November 2017), 1–13. https://doi.org/10.1016/j.trc.2018.11.008

- Krajzewicz, D., Erdmann, J., Behrisch, M., & Bieker, L. (2012). Recent development and applications of SUMO-simulation of urban MObility. *International Journal on Advances in Systems and Measurements*, 5(3&4).
- Kumar, R. R., Chakraborty, A., & Mandal, P. (2021). Promoting electric vehicle adoption: Who should invest in charging infrastructure? Transportation Research Part E: Logistics and Transportation Review, 149(April), Article 102295. https://doi.org/ 10.1016/i.tre.2021.102295
- Liu, X., Sun, X., Zheng, H., & Huang, D. (2021). Do policy incentives drive electric vehicle adoption? Evidence from China. Transportation Research Part A: Policy and Practice, 150(May), 49–62. https://doi.org/10.1016/j.tra.2021.05.013
- Lopez, N. S., Allana, A., & Biona, J. B. M. (2021). Modeling electric vehicle charging demand with the effect of increasing evses: A discrete event simulation-based model. *Energies*, 14(13), 1–15. https://doi.org/10.3390/en14133734
- Macal, C. M., & North, M. J. (2009). Agent-based modeling and simulation. In Proceedings of the 2009 winter simulation conference (WSC) (pp. 86–98).
- Maciejewski, M., & Nagal, K. (2007). Simulation and dynamic optimization of taxi services in MATSim. Europe, 79, 21. https://doi.org/10.1287/xxxx.0000.0000
- Marmaras, C., Xydas, E., & Cipcigan, L. (2017). Simulation of electric vehicle driver behaviour in road transport and electric power networks. *Transportation Research Part C: Emerging Technologies*, 80, 239–256. https://doi.org/10.1016/j. tex.2017.05.004.
- McKinsey. (2019). Expanding electric vehicle adoption despite early growing pains. McKinsey & Company, August.
- Nansai, K., Tohno, S., Kono, M., Kasahara, M., & Moriguchi, Y. (2001). Life-cycle analysis of charging infrastructure for electric vehicles. *Applied Energy*, 70(3), 251–265. https://doi.org/10.1016/S0306-2619(01)00032-0
- US Department of Energy. (2022). New Plug-in Electric Vehicle Sales. https://www.energy.gov/energysaver/articles/new-plug-electric-vehicle-sales-united-states-nearly-doubled-2020-2021, 2022.
- Novosel, T., Perković, L., Ban, M., Keko, H., Pukšec, T., Krajačić, G., & Duić, N. (2015). Agent based modelling and energy planning - utilization of MATSim for transport energy demand modelling. *Energy*, 92, 466–475. https://doi.org/10.1016/j. energy.2015.05.091
- Ou, S., Lin, Z., He, X., & Przesmitzki, S. (2018). Estimation of vehicle home parking availability in China and quantification of its potential impacts on plug-in electric vehicle ownership cost. *Transport Policy*, 68(April), 107–117. https://doi.org/ 10.1016/i.tranpol.2018.04.014
- Paoli, L., & Gill, T. (2022). Electric cars fend off supply challenges to more than double global sales
- Paul, B. M., Doyle, J., Stabler, B., Freedman, J., & Bettinardi, A. (2018). Multi-level population synthesis using entropy maximization-based simultaneous list balancing. Transportation Research Board 93rd Annual Meeting. January 12-16, Washington, D.C. (Vol. 4457(785), pp. 1–19)
- Plugin America. (2016). https://pluginamerica.org/how-much-does-it-cost-charge-electric-car/.
- Seneviratne, P. N. (1985). Acceptable walking distances in central areas. *Journal of Transportation Engineering*, 111(4), 365–376.
- Sheppard, C., Waraich, R., Campbell, A., Pozdnukov, A., & Gopal, A. R. (2017). Modeling plug-in electric vehicle charging demand with BEAM: The framework for behavior energy autonomy mobility. In *Lawrence Berkeley national lab*. Berkeley, CA (United States): LBNI.
- Smart, J., & Schey, S. (2012). Battery electric vehicle driving and charging behavior observed early in the EV project. SAE Technical Papers, 1(1), 27–33. https://doi.org/ 10.4271/2012-01-0199
- Smith, L., Beckman, R., & Baggerly, K. (1995). TRANSIMS: Transportation analysis and simulation system.

- Triplett, T., Santos, R., Rosenbloom, S., & Tefft, B. (2016). *American driving survey* 2014–2015. American Driving Survey. September, 2014–2015 www.aaafoundation.
- Tu, W., Li, Q., Fang, Z., Shaw, S. L., Zhou, B., & Chang, X. (2016). Optimizing the locations of electric taxi charging stations: A spatial-temporal demand coverage approach. Transportation Research Part C: Emerging Technologies, 65(3688), 172–189. https://doi.org/10.1016/j.trc.2015.10.004
- United States Census Bureau. (2019). https://www.census.gov/programs-surveys/acs/microdata.html.
- Vazifeh, M. M., Zhang, H., Santi, P., & Ratti, C. (2019). Optimizing the deployment of electric vehicle charging stations using pervasive mobility data. *Transportation Research Part A: Policy and Practice*, 121(September 2018), 75–91. https://doi.org/ 10.1016/i.tra.2019.01.002
- Wang, K., & Ke, Y. (2018). Public-private partnerships in the electric vehicle charging infrastructure in China: An illustrative case study. Advances in Civil Engineering, 2018. https://doi.org/10.1155/2018/9061647
- Wang, Y., Huang, S., & Infield, D. (2014). Investigation of the potential for electric vehicles to support the domestic peak load. In 2014 IEEE international electric vehicle conference, IEVC 2014. https://doi.org/10.1109/IEVC.2014.7056124
- Wang, Y., & Infield, D. (2018). Markov chain Monte Carlo simulation of electric vehicle use for network integration studies. *International Journal of Electrical Power & Energy Systems*, 99(March 2017), 85–94. https://doi.org/10.1016/j.ijepes.2018.01.008
 Wasatch Front Regional Council. (2021). http://wfrc.org.
- Wu, Y., Ravey, A., Chrenko, D., & Miraoui, A. (2019). Demand side energy management of EV charging stations by approximate dynamic programming. *Energy Conversion* and Management, 196(April), 878–890. https://doi.org/10.1016/j. energy 2010.06.058
- Xi, X., Sioshansi, R., & Marano, V. (2013). Simulation-optimization model for location of a public electric vehicle charging infrastructure. *Transportation Research Part D: Transport and Environment*, 22, 60–69. https://doi.org/10.1016/j.trd.2013.02.014
- Yang, J., Dong, J., & Hu, L. (2018). Design government incentive schemes for promoting electric taxis in China. *Energy Policy*, 115(2), 1–11. https://doi.org/10.1016/j. enpol 2017 12 030
- Yi, Z., Liu, X. C., & Wei, R. (2022). Electric vehicle demand estimation and charging station allocation using urban informatics. *Transportation Research Part D: Transport* and Environment, 106(April), Article 103264. https://doi.org/10.1016/j. trd.2022.103264
- Yi, Z., Liu, X. C., Wei, R., Chen, X., & Dai, J. (2021). Electric vehicle charging demand forecasting using deep learning model. *Journal of Intelligent Transportation Systems*, 1–14
- Yi, Z., & Bauer, P. H. (2016). Optimization models for placement of an energy-aware electric vehicle charging infrastructure. *Transportation Research Part E: Logistics and Transportation Review*, 91, 227–244. https://doi.org/10.1016/j.tre.2016.04.013
- Zhang, Y., Luo, X., Qiu, Y., & Fu, Y. (2022). Understanding the generation mechanism of BEV drivers' charging demand: An exploration of the relationship between charging choice and complexity of trip chaining patterns. *Transportation Research Part A: Policy and Practice*, 158(March), 110–126. https://doi.org/10.1016/j. tra 2022.02.007
- Zheng, J., Wang, X., Men, K., Zhu, C., & Zhu, S. (2013). Aggregation model-based optimization for electric vehicle charging strategy. *IEEE Transactions on Smart Grid*, 4 (2), 1058–1066. https://doi.org/10.1109/TSG.2013.2242207
- Zou, Y., Wei, S., Sun, F., Hu, X., & Shiao, Y. (2016). Large-scale deployment of electric taxis in Beijing: A real-world analysis. *Energy*, 100, 25–39. https://doi.org/10.1016/ j.energy.2016.01.062